Third-order optical nonlinearity in charge-transfer-type conjugated polymers

Hideo Kishida,[1,2] Keisuke Hirota,[1] Takeru Wakabayashi,[1] Ban-Lee Lee,[3] Hisashi Kokubo,[3] Takakazu Yamamoto,[3] and Hiroshi Okamoto[1]

[1]*Department of Advanced Materials Science, University of Tokyo, Kashiwa, Chiba 277-8561, Japan*

[2]*Structural Ordering and Physical Properties Group, PRESTO, JST, Kashiwa 277-8561 Japan*

[3]*Chemical Resources Laboratory, Tokyo Institute of Technology, Yokohama 226-8503, Japan*

(Received 16 April 2004; published 13 September 2004)

We have studied third-order nonlinear optical (NLO) properties of charge-transfer- (CT) type conjugated copolymer composed of an electron-donating molecule, thiophene, and electron-accepting one, quinoxaline, using the electroabsorption, two-photon absorption, and third-harmonic generation spectroscopies. The analyses of the obtained nonlinear optical spectra reveal that the CT character of the excited states leads to small oscillator strength of linear absorption but large third-order nonlinear susceptibility, resulting in the strong enhancement of figure of merit for NLO devices.

DOI: 10.1103/PhysRevB.70.115205 PACS number(s): 78.66.Qn, 78.20.Jq, 42.65.Ky

Since Sauteret *et al.* reported the enhancement of optical nonlinearity in polydiacetylenes due to one-dimensional (1D) confinement of electrons,[1] third-order nonlinear optical (NLO) properties of conjugated polymers have been extensively studied.[2] Many theoretical approaches have also been tried to explain the mechanism of the NLO properties in conjugated polymers.[3–5] Among them, Dixit *et al.*[4] proposed a simple description of the electronic states of conjugated polymers based on the Peierls-extended Hubbard model. Their model is successful in explaining various optical processes in conjugated systems, including not only nonlinear optical processes but also the dynamical behaviors of photoexcited states.[6–14] According to their model, third-order optical nonlinearity in conjugated polymers is dominated by three essential states, which are a ground state $|G\rangle$, a one-photon allowed state $|B\rangle$ with odd parity, and a one-photon forbidden state $|A\rangle$ with even parity. As for linear optical response, most of oscillator strength from the ground state is concentrated on the $|G\rangle$-to-$|B\rangle$ transition with the transition dipole moment expressed as $\langle G|x|B\rangle$. The state $|A\rangle$, which lies immediately above the state $|B\rangle$, closely relates to third-order nonlinear optical response as well as the state $|B\rangle$. It has been suggested that these features are essentially independent of physical parameters dominating electronic structure such as on-site and nearest-neighbor Coulomb repulsions and strength of bond alternations.

Both the excited states, $|B\rangle$ and $|A\rangle$, in conjugated polymers are considered 1D excitons, which have the intermediate character between Wannier and molecular (Frenkel) excitons.[15,16] The natures of these two exciton states, $|B\rangle$ and $|A\rangle$, are considerably different; the state $|B\rangle$ is strongly bound exciton and the state $|A\rangle$ is rather delocalized one. As a result, $\langle G|x|B\rangle$ becomes very large, while $\langle B|x|A\rangle$ is not so increased due to the different spatial extension of the states $|B\rangle$ and $|A\rangle$. The large $\langle G|x|B\rangle$ increases not only the third-order nonlinear susceptibility $\chi^{(3)}$ but also the linear absorption coefficient α, so that it does not necessarily enhance the figure of merit (FOM) for NLO devices defined as $\chi^{(3)}/\alpha$. Therefore, large $\langle B|x|A\rangle$ will be desirable for good NLO materials. The enhancement of $\langle B|x|A\rangle$ is expected to be achieved by making the state $|B\rangle$ as delocalized as the state $|A\rangle$.

A possible approach for this is to introduce charge-transfer (CT) character into the lowest exciton in conjugated polymers. Recently such CT-type polymers have been synthesized, in which electron-donating aromatic molecules and electron-accepting ones are alternately bonded to compose conjugated chains.[17–19] In these copolymers, the optical gap corresponds to the CT transition from the highest occupied molecular orbital (HOMO) of donor to the lowest unoccupied molecular orbital (LUMO) of acceptor. It is expected that the CT character will make the state $|B\rangle$ delocalized. This will lead to the enhancement of $\langle B|x|A\rangle$ through the resemblance of the spatial extension of wave functions of the two excited states.

In this paper, we report the third-order NLO properties of a CT-type copolymer composed of electron-donating molecule, thiophene (Th), and electron-accepting one, quinoxaline (Qx), poly(2,3-bis-(3-octyloxyphenyl)quinoxaline-5, 8-diyl-alt-thiophene-2,5-diyl) (PThQx) [see Fig. 1(a)]. To reveal the effect of the introduction of the CT character, we have performed comparative studies of NLO properties between PThQx and homopolymer, poly(3-hexylthiophene) (PTh) (see Fig. 1(b)), using electroabsorption (EA), two-photon absorption (TPA), and third-harmonic generation (THG) spectroscopies. The EA and TPA spectra reveal the

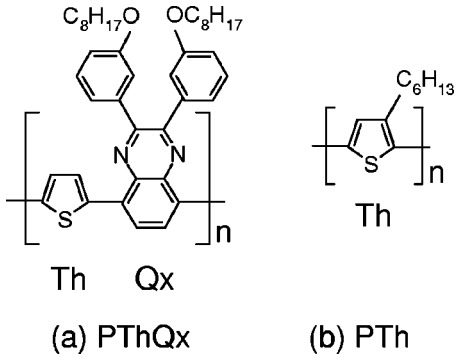

FIG. 1. Molecular structures of PThQx (a) and PTh (b).

overall excited-level structure including one-photon forbidden states, dominating the NLO responses. Moreover, we quantitatively evaluate the third-order nonlinear susceptibility $\chi^{(3)}(-3\omega;\omega,\omega,\omega)$ by THG measurements. From the analysis of $\chi^{(3)}(-3\omega;\omega,\omega,\omega)$ spectra based on a simple discrete-level model, we evaluate the transition dipole moments between the odd and even excited states as well as the oscillator strength of the transition from the ground state to the lowest odd excited state. Comparison of the transition dipole moments and the oscillator strength between PThQx and PTh reveals that the introduction of the CT character to the lowest excited state enhances the FOM for the NLO devices in PThQx.

PThQx is synthesized from two monomers, 2,5-bis(trimethylstannyl)thiophene and 2,3-bis(3-octyloxyphenyl)-5,8-dibromoquinoxalines by organometallic polycondensation. The synthetic method was previously reported in detail.[17] The head-to-tail poly(3-hexylthiophene) (HT-PTh) and random poly(3-hexylthiophenes) (Ra-PTh) are synthesized by the method reported in Refs. 20 and 21, respectively. In Ra-PTh, 20% of Th-Th couplings are of head-to-head type, making the chain regiorandom.

The spin-cast films of PThQx and PTh are fabricated from $CHCl_3$ solution onto SiO_2 substrates. For the EA experiments, we used the film spin-cast onto an ITO-coated SiO_2 substrate, on which a semitransparent aluminum electrode is evaporated. The alternating voltage (frequency $f=1$ kHz) is applied between the ITO and the electrode. The $2f$ component in the change of absorbance is picked up by a lock-in amplifier. To obtain TPA spectrum, the excitation profile of two-photon excited luminescence was measured on PThQx and Ra-PTh by varying the excitation photon energy from 0.73 to 1.3 eV and monitoring the luminescence intensity at a fixed energy, 1.75 eV, which is close to the peak of the luminescence spectrum in both polymers. In the THG experiments, an OPO laser pumped by a Nd:YAG laser was used as a light source (900–2100 nm, pulse width ~6 ns). Third-order nonlinear susceptibility $\chi^{(3)}(-3\omega;\omega,\omega,\omega)$ is obtained by the Maker's fringe method.[22] A sample is mounted in a vacuum cell to avoid the THG from air. A SiO_2 plate was used as a reference sample. All the optical measurements were performed at room temperature (RT) except for the EA measurement of HT-PTh done at 77 K in which the measurement is difficult at RT due to the low resistivity.

Figure 2(a) shows the absorption spectrum of PThQx, which has three peaks labeled by I, II, and III. The lowest absorption peak I is located around 2 eV. This energy is lower than both of the peak energies of homopolymers, PTh (2.4 eV) and polyquinoxaline (PQx) (3.5 eV).[23] Such a low energy shift of the peak I indicates the CT character of the lowest excited state in the copolymer. Namely, the peak I corresponds to the CT transition from the HOMO of the donor (Th) to the LUMO of the acceptor (Qx) with odd parity. The peaks II (3.41 eV) and III (4.35 eV) can be assigned to the intramolecular (IM) HOMO-LUMO transitions of Qx and Th, respectively. In HT-PTh, most of the oscillator strength concentrates on the absorption peak around 2.4 eV, as seen in Fig. 2(d). That is in contrast with PThQx, in which the higher-lying absorption peaks II and III have large absorption coefficients comparable to the lowest peak I.

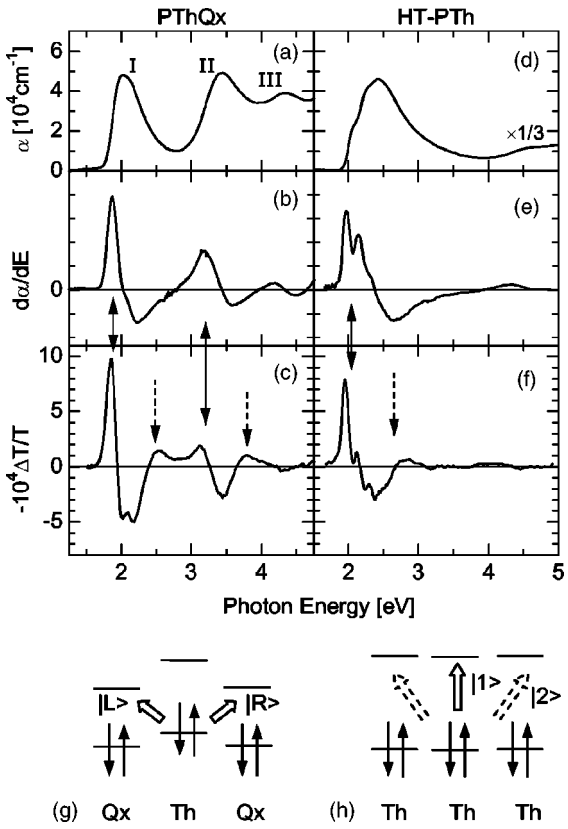

FIG. 2. Absorption coefficient (α) spectra [(a) and (d)], energy-derivative of α [(b) and (e)], and EA spectra [(c) and (f)] of PThQx and HT-PTh, respectively. In (c) and (f), solid-line arrows show the structure corresponding to the Stark shift of the one-photon allowed state. Broken-line arrows to the electric-field induced absorption of one-photon forbidden state. Schematics of the lowest two excited states in PThQx and PTh are shown in (g) and (h), respectively.

EA measurements are useful to investigate the overall energy-level structure in the excited states including one-photon forbidden states with even parity. The EA spectrum of PThQx is shown in Fig. 2(c), in which two oscillating structures are observed around 2 and 3.5 eV. To understand the origin of these structures, we first compare the EA spectrum with the energy-derivative of absorption coefficient, $d\alpha/\mathrm{dE}$ [Fig. 2(b)], which corresponds to the Stark shifts of the one-photon allowed states with odd parity to the lower energy. The lower-energy part of each oscillating structure indicated by the solid-line arrows in the EA spectrum is almost reproduced by $d\alpha/\mathrm{dE}$. However, each oscillating structure has a discrepant positive component in the higher energy part indicated by the dotted-line arrows. As observed in various conjugated polymers,[6,7,9,14,24–29] applied electric field mixes the one-photon allowed state with odd parity and the one-photon forbidden state with even parity, and makes the latter weakly allowed. Therefore, the emergent positive component around 2.5 eV is attributable to the CT excited state with even parity. It is natural to consider that the two CT states with odd and even parity correspond to the above-mentioned *essential states*, $|\mathrm{B}\rangle$ and $|\mathrm{A}\rangle$, respectively. Another positive component around 3.7 eV is reasonably assigned to the IM excited state with even parity.

The absorption spectrum, the first energy-derivative of the absorption $d\alpha/\mathrm{dE}$ and the EA spectrum in HT-PTh are presented in Fig. 2(d)–2(f), respectively. The EA spectrum shows a single oscillating structure at 2–3 eV. As in the case of PThQx, the lower energy part of the oscillating structure indicated by the solid-line arrow is reproduced by $d\alpha/\mathrm{dE}$ and, therefore, can be assigned to the Stark shift. The positive signal observed in the higher energy part indicated by the dotted-line arrow reflects the one-photon forbidden state with even parity. These two states are regarded as the *essential states*. Above 3 eV, no other signal is observed in the EA spectrum of HT-PTh. It is in contrast with the results of PThQx, in which the higher-lying excited states above 3.5 eV show significant contribution to the NLO susceptibility.

The *essential excited states* of PThQx and HT-PTh deduced from the EA measurements are schematically drawn in Figs. 2(g) and 2(h), respectively, by means of a simple localized picture. In this picture, the lowest one-photon allowed excited state ($|1\rangle$) in PThQx, which is observed in the absorption spectrum, is the odd linear combination of the leftward and rightward CT excited states, $|\mathrm{L}\rangle$ and $|\mathrm{R}\rangle$, while the one-photon forbidden excited state ($|2\rangle$) observed in the EA spectrum as the field-induced absorption is their even linear combination. On the other hand, in HT-PTh, the state $|1\rangle$ is the exciton with an electron and a hole located on the same site and the state $|2\rangle$ is a CT state composed of the even combination of the rightward and leftward CT states as shown in Fig. 2(h).

To detect the one-photon forbidden states with even parity more directly, we have performed TPA experiments in PThQx. The obtained spectrum is shown in Fig. 3(a) by the open circles. A distinct peak is observed at 1.24 eV in fundamental photon energy, indicating that the state $|2\rangle$ is located at 2.48 eV. For comparison, we show the TPA spectrum of Ra-PTh in Fig. 3(b) by the open circles. With an increase of energy, the TPA starts to increase at about 1.1 eV and is accompanied by a shoulder structure around 1.2 eV. The shoulder structure and the background component are attributable to TPA to the state $|2\rangle$ and the continuum, respectively, since the one-photon forbidden exciton state is usually located very close to the edge of the continuum in conjugated polymers.[3]

In Fig. 3(a), the THG spectrum of PThQx is shown by the filled circles. It has two prominent structures around 0.65 eV and 1.05 eV in fundamental photon energy. The energy position of the lower peak (0.65 eV) is just one third of the peak energy (1.95 eV) of the absorption spectrum, so that we reasonably attributed this peak to the three-photon resonance to the state $|1\rangle$ [P1 in Fig. 3(c)]. As for the 1.05-eV peak, there are two possible interpretations of resonant structures. One is the two-photon resonance to the state $|2\rangle$ (P2) and another is the three-photon resonance to the higher-lying one-photon allowed IM state $|3\rangle$ (P3). These two processes are not exclusive alternative, but may coexist. In order to clarify the contribution of the two resonant processes, we have fitted the $\chi^{(3)}$ spectrum by using the following equation,[30] including the odd ($|1\rangle$) and even ($|2\rangle$) CT states, and the odd ($|3\rangle$) and even ($|4\rangle$) IM states

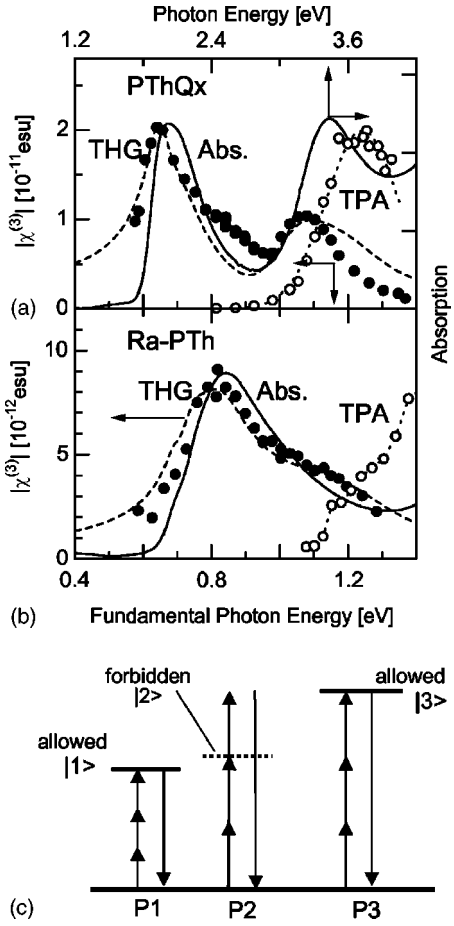

FIG. 3. THG spectra (dots), absorption spectra (solid lines), and TPA spectra (open circles) of PThQx (a) and Ra-PTh (b). The broken lines show the THG spectra calculated based on the discrete-level models. The dotted lines are drawn as guide to eyes for TPA spectra. Figure (c) shows schematically the resonant processes in THG (P1: the three-photon resonance to the state $|1\rangle$, P2:the two-photon resonance to the state $|2\rangle$, and P3: the three-photon resonance to the state $|3\rangle$).

$$\chi^{(3)}(-3\omega;\omega,\omega,\omega) \approx \frac{N}{\epsilon_0}\frac{e^4}{\hbar^3}\left[\frac{\langle 0|x|1\rangle\langle 1|x|2\rangle\langle 2|x|1\rangle\langle 1|x|0\rangle}{(\omega_1 - i\Gamma_1 - 3\omega)(\omega_2 - i\Gamma_2 - 2\omega)(\omega_1 - i\Gamma_1 - \omega)} + \frac{\langle 0|x|3\rangle\langle 3|x|4\rangle\langle 4|x|3\rangle\langle 3|x|0\rangle}{(\omega_3 - i\Gamma_3 - 3\omega)(\omega_4 - i\Gamma_4 - 2\omega)(\omega_3 - i\Gamma_3 - \omega)}\right]. \quad (1)$$

Here, N is the density of aromatic molecules; ω_i and Γ_i are the energy and the damping constant of the state $|i\rangle$, respectively. In Eq. (1), only the two main terms are presented and the other six subsidiary terms are omitted for simplicity. The first and second terms represent the NLO process associated with the CT and IM excited states, respectively. Since the natures of the CT excited states and the IM excited states are considerably different from each other, the transitions between these two kinds of excited states are neglected. In the fitting procedure, it was found that the absorption band I in Fig. 2(a) cannot be explained by a single band due to the presence of a phonon side-band related to the

C=C stretching mode. Considering that the absorption band I is composed of the zero phonon line of the lowest one-photon allowed CT state (the state $|1\rangle$) and its phonon side-band (the state $|1'\rangle$), the absorption band I can be well reproduced. In this case, two CT states $|2\rangle$ and $|2'\rangle$ corresponding to $|1\rangle$ and $|1'\rangle$, respectively, should be considered for the one-photon forbidden CT state as well. However, these two bands could not be distinguished in our NLO spectra. This is possibly due to the broadening of the spectral shape related with $|2\rangle$ and $|2'\rangle$. Therefore, in our analysis, we consider only a single state $|2\rangle$ for the one-photon forbidden CT state and assume that $\langle 1|x|2\rangle = \langle 1'|x|2\rangle$. The calculated spectrum obtained by using the complete expression of $\chi^{(3)}$ is presented by the broken line in Fig. 3(a), which reproduces well the experimental $\chi^{(3)}$ spectrum. The obtained parameters are $\omega_1 = 1.95$ eV, $\omega_{1'} = 2.1$ eV, $\omega_2 = 2.48$ eV, $\omega_3 = 3.1$ eV, $\omega_4 = 3.47$ eV, $\langle 0|x|1\rangle = 0.59$ Å, $\langle 0|x|1'\rangle = 0.695$ Å, $\langle 1|x|2\rangle = \langle 1'|x|2\rangle = 11.2$ Å, $\langle 0|x|3\rangle = 0.803$ Å, $\langle 3|x|4\rangle = 15.5$ Å. The higher-energy peak cannot be explained by the two-photon resonance to the state $|2\rangle$ nor the three-photon resonance to the excited state $|3\rangle$ alone, but can be reproduced by the superposition of these two resonance processes.

In Fig. 3(b), we present the THG spectrum of Ra-PTh by the filled circles, which is considerably different from that of PThQx. The THG spectrum of Ra-PTh shows a single peak at around 0.8 eV and a shoulder structure at around 1.2 eV, which can be reproduced only by the first term in Eq. (1) as shown by the broken line in Fig. 3(b). In this fitting calculation, two phonon side-bands, $|1'\rangle$ and $|1''\rangle$, related to the C=C stretching mode were taken into account as in the case of PThQx. The obtained parameters are $\omega_1 = 2.08$ eV, $\omega_{1'} = 2.26$ eV, $\omega_{1''} = 2.44$ eV, $\omega_2 = 2.4$ eV, $\langle 0|x|1\rangle = 0.16$ Å, $\langle 0|x|1'\rangle = 0.53$ Å, $\langle 0|x|1''\rangle = 0.95$ Å, $\langle 1|x|2\rangle = \langle 1'|x|2\rangle = \langle 1'|x|2\rangle = 4.9$ Å. The main peak and the shoulder structure of the $\chi^{(3)}$ spectrum are attributable to the three-photon resonance to the one-photon allowed state and the two-photon resonance to the one-photon forbidden state.

The maximum value of $\chi^{(3)}$ in PThQx reaches 2×10^{-11} esu, which is larger than that of Ra-PTh (0.9×10^{-11} esu). In order to clarify the difference of the NLO response between PThQx and PTh, we compare the obtained parameters of the two polymers in Fig. 4. The oscillator strength f of linear absorption per aromatic unit (Th or Qx) in PThQx is 0.43, which is much smaller than that of PTh (0.76). As for $\langle 1|x|2\rangle$, PThQx shows a larger value (11.2 Å) than PTh (4.9 Å). Taking into account the spatial configuration of an electron and a hole in the excited state, we can deduce that the CT copolymer has smaller f and larger $\langle 1|x|2\rangle$ as follows. In the exciton picture, the magnitude of f is determined by the amplitude of the envelope function of the exciton at the origin in the relative coordinate between the excited electron and hole.[31] The amplitude at the origin corresponds to the probability of the on-site or the IM excitation. Therefore, the CT copolymer has relatively small f as compared with the homopolymer. On the other hand, $\langle 1|x|2\rangle$ is dominated by the similarity in the spatial extention of the envelope functions between these two excited states. In the CT copolymer, their envelope functions will be similar to each other except for the symmetry because both states essentially have the CT character. It results in the enhancement of $\langle 1|x|2\rangle$. As shown in Eq. (1), $\chi^{(3)}(-3\omega;\omega,\omega,\omega)$ is proportional to $\langle 0|x|1\rangle^2\langle 1|x|2\rangle^2$ and therefore to $f\langle 1|x|2\rangle^2$. In PThQx, $\chi^{(3)}$ is enhanced as compared with Ra-PTh, since the increase of $\langle 1|x|2\rangle$ overcomes the decrease of f.

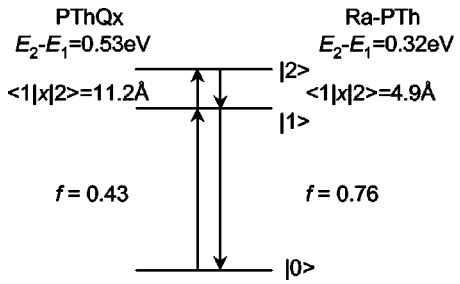

FIG. 4. Comparison of the parameters concerning the linear and nonlinear optical responses between PThQx and Ra-PTh.

In applications of NLO materials to optical switching devices, the third-order NLO process represented by $\chi^{(3)}(-\omega;\omega,-\omega,\omega)$ is used. This $\chi^{(3)}$ is not reported in this paper. However, the magnitude can be discussed because it is governed by $f\langle 1|x|2\rangle^2$, as is the case with $\chi^{(3)}(-3\omega;\omega,\omega,\omega)$. Considering the large $\chi^{(3)}(-3\omega;\omega,\omega,\omega)$ in PThQx, $\chi^{(3)}(-\omega;\omega,-\omega,\omega)$ will be also large in PThQx. The figure of merit (FOM) for optical switching devices is usually described by $\chi^{(3)}(-\omega;\omega,-\omega,\omega)/\alpha$, which should be enhanced further in PThQx, since the CT character of the lowest exciton state in PThQx leads to the decrease of f and therefore the decrease of α. From these results, we can demonstrate the following strategy to enhance the magnitude of the FOM for NLO materials; the FOM should be enhanced by strengthening the CT character in copolymers, which is achieved by increasing the electron-donating character of donor molecules and the electron-accepting character of acceptors.

In summary, we have investigated NLO properties of a CT copolymer, PThQx. On the basis of the EA and TPA spectra, we have demonstrated that one-photon forbidden CT state with even parity located just above the one-photon allowed CT state with odd parity plays an important role in the NLO response. The THG measurements showed that the maximum value of $\chi^{(3)}$ reaches 2×10^{-11} esu in PThQx, which is larger than that (0.9×10^{-11} esu) of Ra-PTh. The analysis of the THG spectrum as well as of the absorption spectrum reveals that the transition dipole moment between the two CT excited states is enhanced, while that between the ground state and the one-photon allowed CT state is suppressed in PThQx, as compared with Ra-PTh. These features will lead to the enhancement of FOM for NLO devices in PThQx.

[1] C. Sauteret, J.-P. Hermann, R. Frey, F. Pradère, J. Ducing, R. H. Baughman, and R. R. Chance, Phys. Rev. Lett. **36**, 956 (1976).
[2] H. S. Nalwa, Adv. Mater. (Weinheim, Ger.) **5**, 341 (1993).
[3] Z. G. Soos and S. Ramasesha, J. Chem. Phys. **90**, 1067 (1989).
[4] S. N. Dixit, D. Guo, and S. Mazumdar, Phys. Rev. B **43**, 6781 (1991).
[5] S. Mukamel and H. X. Wang, Phys. Rev. Lett. **69**, 65 (1992).
[6] J. M. Leng, S. Jeglinski, X. Wei, R. E. Benner, Z. V. Vardeny, F. Guo, and S. Mazumdar, Phys. Rev. Lett. **72**, 156 (1994).
[7] F. Rohlfing and D. D. C. Bradley, Chem. Phys. Lett. **277**, 406 (1997).
[8] M. Ozaki, E. Ehrenfreund, R. E. Benner, T. J. Barton, K. Yoshino, and Z. V. Vardeny, Phys. Rev. Lett. **79**, 1762 (1997).
[9] M. Liess, S. Jeglinski, Z. V. Vardeny, M. Ozaki, K. Yoshino, Y. Ding, and T. Barton, Phys. Rev. B **56**, 15712 (1997).
[10] I. Gontia, S. V. Frolov, M. Liess, E. Ehrenfreund, Z. V. Vardeny, K. Tada, H. Kajii, R. Hidayat, A. Fujii, K. Yoshino, M. Teraguchi, and T. Masuda, Phys. Rev. Lett. **82**, 4058 (1999).
[11] S. V. Frolov, Z. Bao, M. Wohlgenannt, and Z. V. Vardeny, Phys. Rev. Lett. **85**, 2196 (2000).
[12] L. Moroni, P. R. Salvi, C. Gellini, G. Dellepiane, D. Comoretto, and C. Cuniberti, J. Phys. Chem. A **105**, 7759 (2001).
[13] D. Scherer. R. Dörfler, A. Feldner, T. Vogtmann, M. Schwoerer, U. Lawrentz, W. Grahn, and C. Lambert, Chem. Phys. **279**, 179 (2002).
[14] R. Österbacka, M. Wohlgenannt, M. Shkunov, D. Chin, and Z. V. Vardeny, J. Chem. Phys. **118**, 8905 (2003).
[15] H. X. Wang and S. Mukamel, Chem. Phys. Lett. **192**, 417 (1992).
[16] T. Hasegawa, Y. Iwasa, T. Koda, H. Kishida, Y. Tokura, S. Wada, H. Tashiro, H. Tachibana, and M. Matsumoto, Phys. Rev. B **54**, 11365 (1996).
[17] T. Yamamoto, Z. H. Zhou, T. Kanbara, M. Shimura, K. Kizu, T. Maruyama, Y. Nakamura, T. Fukuda, B. L. Lee, N. Ooba, S. Tomaru, T. Kurihara, T. Kaino, K. Kubota, and S. Sasaki, J. Am. Chem. Soc. **118**, 10389 (1996).
[18] B. L. Lee and T. Yamamoto, Macromolecules **32**, 1375 (1999).
[19] T. Yamamoto, B. L. Lee, H. Kokubo, H. Kishida, K. Hirota, T. Wakabayashi, and H. Okamoto, Macromol. Rapid Commun. **24**, 440 (2003).
[20] T.-A. Chen, X. Wu, and R. D. Rieke, J. Am. Chem. Soc. **117**, 233 (1995).
[21] R. Sugimoto, S. Takeda, and K. Yoshino, Chem. Express **1**, 635 (1986).
[22] F. Kajzar and J. Messier, Phys. Rev. A **32**, 2352 (1985).
[23] T. Yamamoto, K. Sugiyama, T. Kushida, T. Inoue, and T. Kanbara, J. Am. Chem. Soc. **118**, 3930 (1996).
[24] Y. Tokura, T. Koda, A. Itsubo, M. Miyabayashi, K. Okuhara, and A. Ueda, J. Chem. Phys. **85**, 99 (1986).
[25] R. G. Kepler and Z. G. Soos, Phys. Rev. B **43**, 12530 (1991).
[26] G. Weiser, Phys. Rev. B **45**, 14076 (1992).
[27] H. Kishida, T. Hasegawa, Y. Iwasa, T. Koda, Y. Tokura, H. Tachibana, M. Matsumoto, S. Wada, T. T. Lay, and H. Tashiro, Phys. Rev. B **50**, 7786 (1994).
[28] K. Sakurai, H. Tachibana, N. Shiga, C. Terakura, M. Matsumoto, and Y. Tokura, Phys. Rev. B **56**, 9552 (1997).
[29] F. Feller and A. P. Monkman, Phys. Rev. B **60**, 8111 (1999).
[30] P. N. Butcher and D. Cotter, *The Elements Of Nonlinear Optics* (Cambridge University Press, Cambridge, 1990).
[31] Y. Toyozawa, *Optical Processes in Solids* (Cambridge University Press, Cambridge, 1999).